532.516 : 621.822.5

Paper No. 211-18

Influence of Gas Inertia Forces Generated Within the Stabilizing Restrictor on Dynamic Characteristics of Externally Pressurized Thrust Gas Bearings*

(2nd Report, Case of Turbulent Flow at the Capillary Restriction)

By Yoshio HARUYAMA**, Tsuneji KAZAMAKI***, Haruo MORI**** and Kenji NAKAGAWA*****

The influence of the gas inertia forces generated within the stabilizing restrictor in capillary form has been discussed about the case of a laminar flow in the first report[1]. *In this paper, we investigated theoretically and experimentally the inertia effect generated within the capillary restricted part in the case of a turbulent flow.*

From comparison with the experiment, it is concluded that the influence on the dynamic characteristics should be considerable, and that the presented analysis yields good predictions of both the bearing stiffness and the damping coefficient in a wide range of designing conditions.

Key Words : Lubrication, Bearing, Externally Pressurized Thrust Bearing, Dynamic Characteristics, Inertia Effect, Capillary Restriction, Turbulent Flow

1. Introduction

In the first report[1], the authors investigated theoretically and experimentally the influence of the gas inertia forces generated within the stabilizing capillary restrictor on the dynamic characteristics of externally pressurized thrust gas bearings and pointed out that the influence should be considerable. It should be noted that the conventional analysis is based on the assumption that the flow of gas from the capillary restriction is a laminar flow and therefore the analysis would be impossible when the Reynolds number becomes large. In fact, the experimental data of the damping coefficient deviate considerably from the theoretical estimations when the supply pressure is high[2]. In this paper, the authors investigated theoretically and experimentally the influence of the gas inertia forces generated within the stabilizing restrictor on the dynamic characteristics for the case when the flow of gas from the capillary restriction becomes turbulent.

The bearing analyzed here is the same externally pressurized circular thrust gas bearing as the one in the first report. The stabilizer is inserted into the gas supply-line.

* Received 8th May, 1981.
** Instructor, Faculty of Engineering, Toyama University, 1-1, Nakagawa-Sonomachi, Takaoka, Japan.
*** Professor, Faculty of Engineering, Toyama University, 1-1, Nakagawa-Sonomachi, Takaoka, Japan.
**** Professor, Faculty of Engineering, Kyoto University, Yoshida-Honmachi, Sakyo-ku, Kyoto, Japan.
***** Graduate student, Graduate School, Toyama University, 1-1, Nakagawa-Sonomachi, Takaoka, Japan.

2. Nomenclature

We use the same symbols as the ones described in the first report, and the new main symboles are added to this paper as follows and furthermore the rest ones are given in thr body of the paper.

c_{D1}, c_{D2} : discharge coefficient
$g \equiv P_{i0}/P_{c0}$
P_i : dimensionless pressure at entrance of capillary restriction
$P_{ir0} = (P_{i0}+P_{r0})/2$
r_{cj} : radius of the boundary between the j'th region and the $(j+1)$'th region
$R_{cj}=r_{cj}/a$
$R^* \equiv u^*a/\nu_0$
$R_e^* \equiv 2a\bar{u}_{m,st}/\nu_0$: Reynolds number
u : axial velocity component
u^* : friction velocity
$y = a - r_c$
$y^* \equiv u^*y/\nu_0$

$$\gamma_1=\frac{8\mu c_{D1}r_s^2\sqrt{\Re T}\,l}{na^4p_a}$$

$$\gamma_2=\frac{c_{D1}r_s^2}{nc_{D2}a^2}$$

$$\delta=\frac{p_aV_c}{12n\pi\mu c_{D2}a^2\sqrt{\Re T}}\left(\frac{h_0}{r_0}\right)^2$$

η : wave propagation constant
λ : coefficient of fluid friction
τ_w: wall shear stress
ν_Σ: modified kinematic eddy viscosity

Subscripts

j : denotes the quantities in the j'th region
m : denotes the cross-sectional mean values
os : denotes the oscillating component due to pulsation
st : denotes the steady component
$^{-}$: denotes the short-time average values

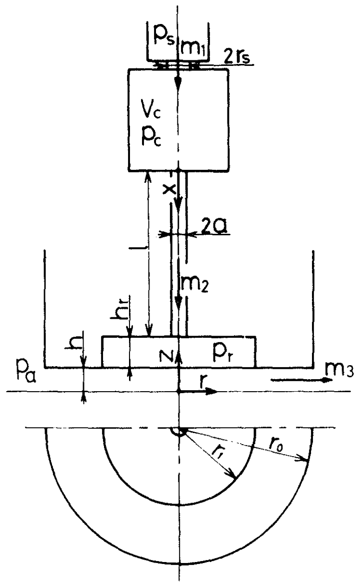

Fig.1 Coordinate system for thrust bearing

3. Theoretical analysis

The externally pressurized circular thrust gas bearing with a stabilizer analyzed in this paper, which is the same bearing as one in the first report, is shown schematically in Fig.1. In the first report, the pressure drop at the entrance of capillary restriction is neglected. It may be necessary to consider a pressure drop, however, when the flow within the capillary has high speed. In this paper, therefore, the pressure drop is evaluated by the formula for the flow through an orifice with the same sectional area as the capillary.

3.1 Assumptions

The following assumptions are used in order to simplify the analysis.

(1) The flow through the bearing gap is viscous so that the variation of gas pressure is ruled by Reynolds equation.

(2) The depth of the recess is large enough compared with the bearing clearance so that the recess pressure may be uniform and it may be equal to the bearing gap pressure at $r=r_1$.

(3) The flow through the capillary restriction is turbulent. The pressure drop at the entrance of capillary is evaluated by the formula for the flow through an orifice with the same sectional area as the capillary and the inlet is so short that it may be neglected.

(4) The change of the state of gas is isothermal.

(5) The thrust plate is paralled to the bearing surface.

3.2 Fundamental equations

The governing equations for the bearing gap pressure are exactly the same equations as those in the first report. Taking a small sinusoidal vibration which occurs around the equilibrium state of bearing into consideration, the dimensionless clearance, H , may be given by

$$H=1+\varepsilon\sin\tau \tag{1}$$

Assuming the dimensionless bearing pressure, P , as

$$P(R,\tau)=P_0(R)+\varepsilon\{P_1(R)\sin\tau+P_2(R)\cos\tau\} \tag{2}$$

we obtain the following fundamental equations for $P_0 \sim P_2$

$$\frac{d}{dR}\left[R\frac{dP_0^2}{dR}\right]=0 \tag{3}$$

$$\frac{1}{R}\frac{d}{dR}\left[R\frac{d(P_0P_1)}{dR}\right]=-\sigma P_2 \tag{4}$$

$$\frac{1}{R}\frac{d}{dR}\left[R\frac{d(P_0P_2)}{dR}\right]=\sigma(P_0+P_1) \tag{5}$$

3.3 Boundary conditions

Adding the condition for the pressure drop at the entrance of capillary restriction to the same conditions as those in the first report, the boundary conditions can be written in the forms,

$$P_0|_{R=1}=1,\quad P_1|_{R=1}=P_2|_{R=1}=0 \tag{6}$$

$$m_2|_{x=0}=m_1-\frac{\partial}{\partial t}(\rho_cV_c) \tag{7}$$

$$m_3|_{r=r_1}=m_2|_{x=l}-\frac{\partial}{\partial t}(\rho_rV_r) \tag{8}$$

$$\frac{c_{D2}\pi a^2p_a}{\sqrt{\Re T}}P_c\phi_2=m_2|_{x=0} \tag{9}$$

where

$$\begin{aligned}\phi_2&=\left(\frac{2\kappa}{\kappa-1}\right)^{1/2}\left(\frac{P_i}{P_c}\right)^{1/\kappa}\left[1-\left(\frac{P_i}{P_c}\right)^{(\kappa-1)/\kappa}\right]^{1/2} &&: \frac{P_i}{P_c}>\left(\frac{2}{\kappa+1}\right)^{\kappa/(\kappa-1)}\\ &=\left(\frac{2\kappa}{\kappa+1}\right)^{1/2}\left(\frac{2}{\kappa+1}\right)^{1/(\kappa-1)} &&: \frac{P_i}{P_c}\leqq\left(\frac{2}{\kappa+1}\right)^{\kappa/(\kappa-1)}\end{aligned} \tag{10}$$

and P_i is a dimensionless pressure at the entrance of capillary restriction. m_1 and m_2 are given by

$$m_1=\frac{c_{D1}\pi r_s^2 p_a}{\sqrt{\Re T}}P_s\phi_1 \tag{11}$$

$$m_3=-\frac{\pi h_0^3 p_a^2}{12\mu\Re T}RH^3\frac{\partial P^2}{\partial R} \tag{12}$$

where

$$\begin{aligned}\phi_1&=\left(\frac{2\kappa}{\kappa-1}\right)^{1/2}\left(\frac{P_c}{P_s}\right)^{1/\kappa}\left[1-\left(\frac{P_c}{P_s}\right)^{(\kappa-1)/\kappa}\right]^{1/2} &&: \frac{P_c}{P_s}>\left(\frac{2}{\kappa+1}\right)^{\kappa/(\kappa-1)}\\ &=\left(\frac{2\kappa}{\kappa+1}\right)^{1/2}\left(\frac{2}{\kappa+1}\right)^{1/(\kappa-1)} &&: \frac{P_c}{P_s}\leqq\left(\frac{2}{\kappa+1}\right)^{\kappa/(\kappa-1)}\end{aligned} \tag{13}$$

We now consider the mass flow rate through stabilizing capillary restriction, m_2 , Unsteady viscous compressible turbulent flow through a straight circular pipe was investigated by Ohmi, et al[3]. We now obtain the mass flow rate, m_2 , by the three region B model in their paper. In this model, the section of pipe is divided into three regions and the modified kinematic eddy viscosity in the j'th region, $\nu_{\Sigma,j}$, is written in the form,

$$\nu_{\Sigma,j}/\nu_0=k_j y^*+n_j \tag{14}$$

where $y^*\equiv u^*y/\nu_0$, $y=a-r_c$, $u^*=\sqrt{\tau_{w,st}/\rho_0}$ and $\tau_{w,st}$ is the wall shear stress in steady flow. The values of k_j and n_j are given by the assumption. For the case of a sinusoidal oscillating flow with angular speed, ω , the pressure and the velocity distributions are given by

(steady component)

$$\bar{p}_{st}=F_0+G_0x \tag{15}$$

$$\frac{\bar{u}_{j,st}}{u^*}=\begin{cases}-\dfrac{R^*}{2(\nu_{\Sigma,j}/\nu_0)}\left(\dfrac{r_c}{a}\right)^2+E_j & (\text{ in the region } k_j=0\ )\\ \dfrac{1}{k_j}\left(\dfrac{r_c}{a}\right)+\left(\dfrac{1}{k_j}+\dfrac{n_j}{R^*k_j^2}\right)\ln(\nu_{\Sigma,j}/\nu_0)+E_j & (\text{ in the region } k_j\neq 0\ )\end{cases} \tag{16}$$

(oscillating component)

$$\bar{p}_{0s}=(Ae^{\eta x}+Be^{-\eta x})e^{i\omega t} \tag{17}$$

$$\bar{u}_{j,os}=\{\eta/(i\omega\rho_0)\}(Ae^{\eta x}-Be^{-\eta x})\{C_jI_0(z_j)+D_jK_0(z_j)-1\}e^{i\omega t} \tag{18}$$

where

$R^*=\dfrac{u^*a}{\nu_0}$, $\eta=\dfrac{i\omega/c_0}{\sqrt{1-\{2/(a\sqrt{i\omega/\nu_0})\}[C_1I_1\{z_1(a)\}-D_1K_1\{z_1(a)\}]}}$: the wave propagation constant,

$z_j(r_c)=r_c\sqrt{i\omega/\nu_{\Sigma,j}}$ (in the region $k_j=0$)

$\quad=2\sqrt{i\omega\nu_{\Sigma,j}}/(k_ju^*)$ (in the region $k_j\neq 0$)

$A, B, C_j, D_j, E_j, F_0, G_0$: integration constants,

I_0, I_1 : modified Bessel functions of the first kind of orders zero and first, respectively,

K_0, K_1 : modified Bessel functions of the second kind of orders zero and first, respectively

and $^-$ denotes the short-time average values (refer to the reference (3)).

Reynolds number $R_e^*=2a\bar{u}_{m,st}/\nu_0$ is related to R^* as $2R^*=R_e^*\sqrt{\lambda/8}$ and the coefficient of fluid friction, λ , is determined only by Re^* in the case of smooth pipe wall. Therefore R^* depends only on Re^*. In this paper, we use

Kármán-Nikuradse formula

$$1/\sqrt{\lambda}=2\log_{10}(R_e^*\sqrt{\lambda})-0.8 \tag{19}$$

as the relation between λ and Re^*.
Assuming P_i and P_r as

$$P_i=P_{i0}+\varepsilon(P_{i1}\sin\tau+P_{i2}\cos\tau) \tag{20}$$

$$P_r=P_{r0}+\varepsilon(P_{r1}\sin\tau+P_{r2}\cos\tau) \tag{21}$$

we get the following equations for $m_2|_{x=0}$ and $m_2|_{x=l}$

$$m_2|_{x=0}=\frac{n\pi a^4 p_a^2}{8\mu\Re Tl}P_{ir0}\{(1-M_0)(P_{i0}-P_{r0})+(M_1P_{i1}+M_2P_{i2}+M_3P_{r1}+M_4P_{r2})\varepsilon\sin\tau$$
$$+(M_1P_{i2}-M_2P_{i1}+M_3P_{r2}-M_4P_{r1})\varepsilon\cos\tau\} \tag{22}$$

$$m_2|_{x=l}=\frac{n\pi a^4 p_a^2}{8\mu\Re Tl}P_{ir0}\{(1-M_0)(P_{i0}-P_{r0})-(M_1P_{r1}+M_2P_{r2}+M_3P_{i1}+M_4P_{i2})\varepsilon\sin\tau$$
$$-(M_1P_{r2}-M_2P_{r1}+M_3P_{i2}-M_4P_{i1})\varepsilon\cos\tau\} \tag{23}$$

where

$$M_0=R_{c1}^4-\frac{1}{k_2R^*}\left\{\frac{k_2R_{c2}^4}{0.07}+\frac{4}{3}(R_{c2}^3-R_{c1}^3)+2(R_{c2}^2-R_{c1}^2)+4(R_{c2}-R_{c1})+4\ln\frac{1-R_{c2}}{1-R_{c1}}\right\} \tag{24}$$

and $M_1 \sim M_4$ are real variables which are determined by the Reynolds number, Re^*, the inertia parameter, $\alpha=\rho_0a^2p_ah_0^2/(12\mu^2r_0^2)$, the compressibility parameter, $\beta=p_alh_0^2/(12\mu c_0r_0^2)$ and the squeeze number, σ.
m_2 is given by treating quasisteadily the flow rate through the capillary as follows

$$m_2=\frac{n\pi a^4p_a^2(1-M_0)}{16\mu\Re Tl}(P_i^2-P_r^2)$$
$$\fallingdotseq\frac{n\pi a^4p_a^2(1-M_0)}{8\mu\Re Tl}\Big[P_{ir0}\{(P_{i0}-P_{r0})+(P_{i1}-P_{r1})\varepsilon\sin\tau+(P_{i2}-P_{r2})\varepsilon\cos\tau\}$$
$$+\frac{P_{i0}-P_{r0}}{2}\{(P_{i1}+P_{r1})\varepsilon\sin\tau+(P_{i2}+P_{r2})\varepsilon\cos\tau\}\Big] \tag{25}$$

Substituting Eqs.(10) ~ (13), (1) and (20) ~ (23) into Eqs.(7) ~ (9), we obtain the following equations as boundary conditions

$$\left.\frac{dP_0^2}{dR}\right|_{R=R_1}=-\frac{\Gamma P_s\phi_{10}}{\phi} \tag{26}$$

$$\gamma_2P_s\phi_{10}=P_{c0}\phi_{20} \tag{27}$$

$$P_{c0}\phi_{20}=\frac{\gamma_2}{\gamma_1}(1-M_0)P_{ir0}(P_{i0}-P_{r0}) \tag{28}$$

$$\left.\frac{d(P_0P_1)}{dR}\right|_{R=R_1}=\frac{\Gamma}{\phi\gamma_1}P_{ir0}\left\{\frac{3}{2}(1-M_0)(P_{i0}-P_{r0})+\frac{1}{2}(M_1P_{r1}+M_2P_{r2}+M_3P_{i1}+M_4P_{i2})\right.$$
$$\left.-\frac{1}{2}\sigma R_1(1+H_r)\frac{P_0P_2}{P_{r0}}\right|_{R=R_1} \tag{29}$$

$$\left.\frac{d(P_0P_2)}{dR}\right|_{R=R_1}=\frac{\Gamma}{2\phi\gamma_1}P_{ir0}(M_1P_{r2}-M_2P_{r1}+M_3P_{i2}-M_4P_{i1})+\frac{1}{2}\sigma R_1\left\{P_{r0}+(1+H_r)\left.\frac{P_0P_1}{P_{r0}}\right|_{R=R_1}\right\} \tag{30}$$

$$P_{c0}A_2\phi_{20}(P_{i1}-gP_{c1})=\gamma_2P_s\phi_{10}A_1P_{c1}-\delta\sigma P_{c2}/2 \tag{31}$$

$$P_{c0}A_2\phi_{20}(P_{i2}-gP_{c2})=\gamma_2P_s\phi_{10}A_1P_{c2}+\delta\sigma P_{c1}/2 \tag{32}$$

$$P_{ir0}(M_1P_{i1}+M_2P_{i2}+M_3P_{r1}+M_4P_{r2})=-2\gamma_1P_{c0}A_2\phi_{20}(P_{i1}-gP_{c1})/\gamma_2 \tag{33}$$

$$P_{ir0}(M_1P_{i2}-M_2P_{i1}+M_3P_{r2}-M_4P_{r1})=-2\gamma_1P_{c0}A_2\phi_{20}(P_{i2}-gP_{c2})/\gamma_2 \tag{34}$$

where

$$\phi_{10}=\phi_1|_{P_c=P_{c0}},\quad \phi_{20}=\phi_2\Big|_{\substack{P_c=P_{c0}\\P_i=P_{i0}}},\quad A_1=\frac{-1}{2\phi_{10}}\left.\frac{\partial\phi_1}{\partial P_c}\right|_{P_c=P_{c0}},\quad A_2=\frac{-1}{2\phi_{20}}\left.\frac{\partial\phi_2}{\partial P_i}\right|_{\substack{P_c=P_{c0}\\P_i=P_{i0}}},\quad g=\frac{P_{i0}}{P_{c0}}$$

$\Gamma=-\frac{12\mu c_{D1}r_s^2\sqrt{\Re T}}{p_ah_0^3}\ln R_1$: the feeding parameter

$$\gamma_1 = \frac{8\mu c_{D1} r_s^2 \sqrt{\Re T}\, l}{n a^4 p_a}$$

$$\gamma_2 = \frac{c_{D1} r_s^2}{n c_{D2} a^2}$$

$$\delta = \frac{p_a V_e}{12 n \pi c_{D2} a^2 \mu \sqrt{\Re T}} \left(\frac{h_0}{r_0}\right)^2$$

$$\psi \equiv -R_1 \ln R_1$$

3.4 Dimensionless stiffness and dimensionless damping coefficient

The bearing pressure, $P_0 \sim P_2$, can be analyzed by solving the fundamental equations, Eqs.(3) ~ (5) under the boundary conditions, Eqs.(6) and (26) ~ (34). P_1 and P_2 are obtained by Runge-Kutta-Gill method, because these are insoluble analytically. The dimensionless stiffness, K, and the dimensionless damping coefficient, B, are defined in the same way as those in the first report. Finally, both K and B can be derived using the eight conventional dimensionless designing parameters : Γ, P_s, R_1, H_r, γ_1, γ_2, δ, σ and three new dimensionless parameter : α (the inertia parameter), β (the compressibility parameter), Re^* (the Reynolds number). The influence of the gas inertia forces within the capillary restriction on the dynamic characteristics can be determined by α, β and Re^*.

In this model for turbulent flow, the Reynolds number, Re^*, must be about 2000 and above[3].

4. Examples of calculated results

Examples of calculated results for R_1=0.5, H_r=10, γ_1=0.2, γ_2=0.2 and δ=100 are given in Figs.2 to 6. In these figures, the theoretical results in which the flow within the capillary restriction is treated quasisteadily are indicated with a broken line.

Figs.2 to 5 show the influence of Re^*, α, β and P_s respectively on K and B. The influence is considerable when Γ takes the values for practical applications from 1 to 10. In general, the inertia effect on B is more remarkable than that on K. Fig.2 gives the influence of Re^* on K and B. In general, the inertia effect becomes remarkable as Re^*decreases in value. Fig.3 gives the influence of α on K and B. In general, the inertia effect becomes remarkable as α increases in value. Fig.5 shows the influence of P_s on K and B. The influence on B becomes significant as P_s increases in value. In general, however, the influence on K of the change of P_s is not so remarkable.

Fig.6 shows the influence of σ on K and B/σ. The influence on B becomes significant when σ decreases in value. In general, however, the

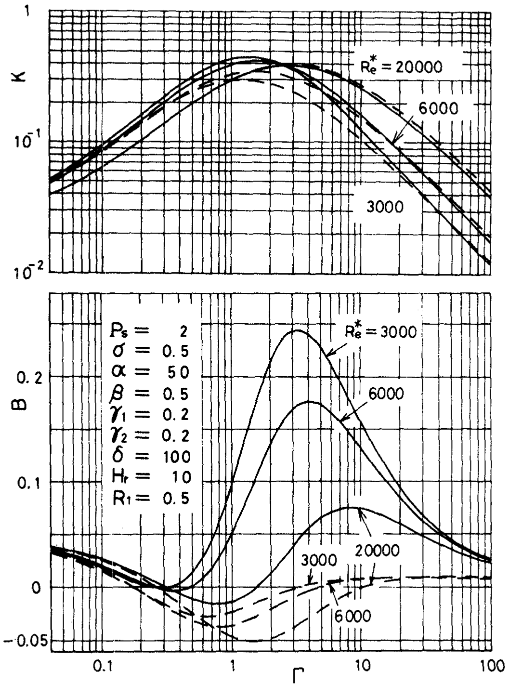

Fig.2 K, B for different Re^*

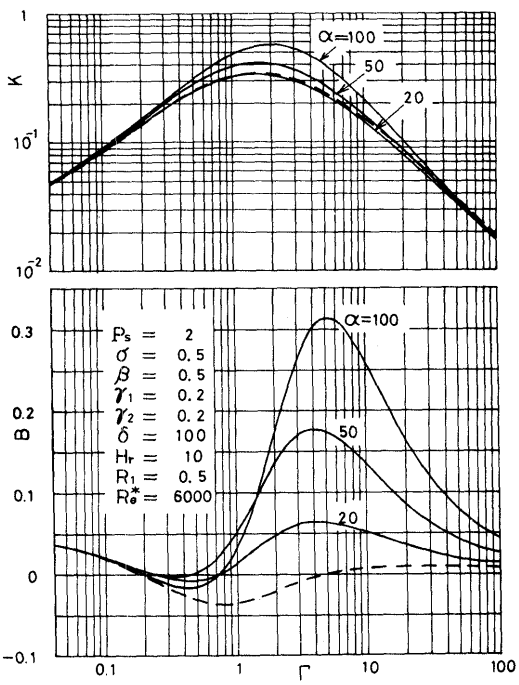

Fig.3 K, B for different α

influence of the inertia forces is not so remarkable when σ is large.

These characteristics are almost in agreement qualitatively with those in the first report.

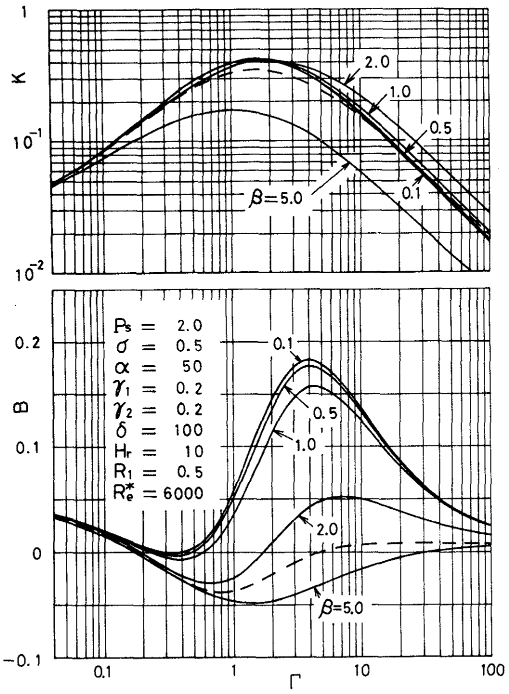

Fig.4 K , B for different β

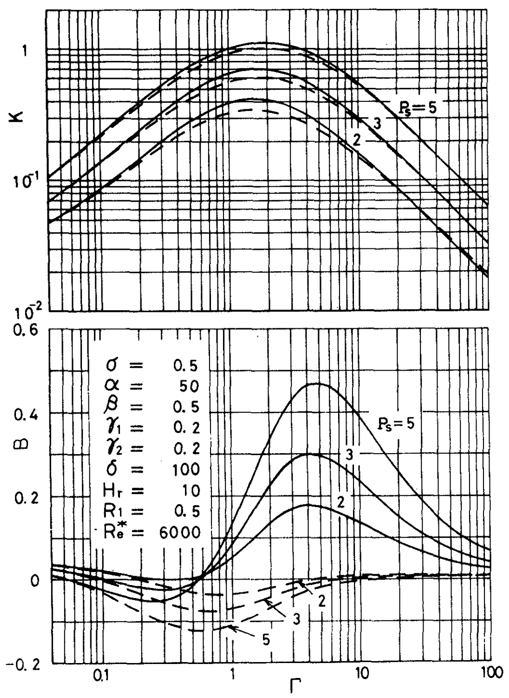

Fig.5 K , B for different P_s

5. Comparison with the experimental results

The experimental apparatus and procedure are the same as reported in the first paper. The shaft is supported by a test thrust bearing, an externally pressurized gas journal bearing and a back pressure of lower volume.

The bearing stiffness and the damping coefficient are obtained by the following method. An impulse load is given to the shaft, while the response to it is recorded by a digital memory,

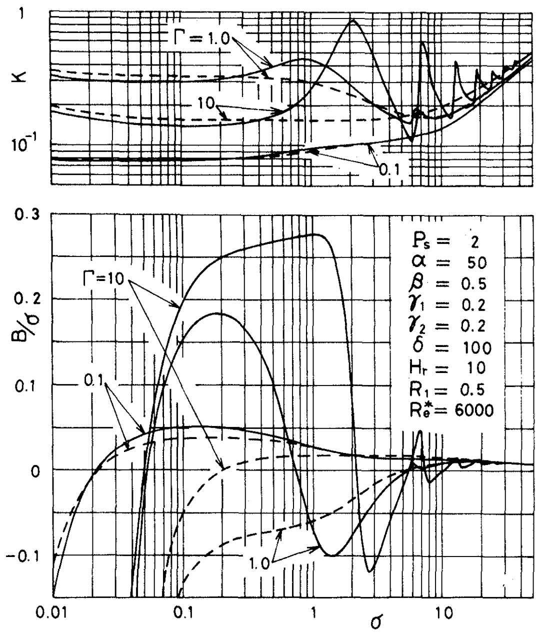

Fig.6 Variation of K , B with squeeze number

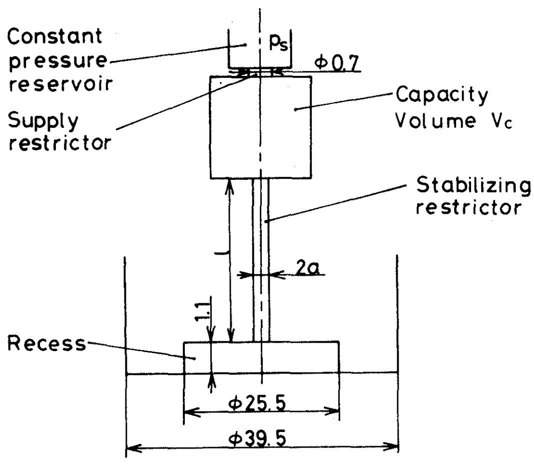

Bearing No.	a mm	l mm	n
1	0.50	200	3
2	0.95	250	1

Fig.7 Dimensions of test bearings

and analyzed by an oscilloscope yielding the logarithmic decrement and frequency of shaft vibration. The stiffness and the damping coefficient are calculated using the logarithmic decrement and frequency. The mass of shaft is 1.50 kg (1.53×10^{-3} kgf s^2/cm).

Details of the test bearing are shown in Fig.7. The supply restrictor consists of an orifice whose diameter is 0.7 mm. The stabilizing restrictor consists of some straight circular pipes whose radius, a , and length, l , are shown in Fig.7. The fluid capacity , V_c , is 100 cm^3.

In Figs.8 and 9, the theoretical estimations of K and B are compared with the experimental results. In these figures, the theoretical results in which the flow within the capillary restriction is treated quasisteadily are indicated with a broken line and those in which the flow within the capillary is treated as a laminar flow(1) are indicated with an alternately long and short dash line. In this experiment, the theoretical Reynolds number within the capillary restriction is 2500 and above. We use Perry's experimental equation(4) as discharge coefficient, c_{D1} , c_{D2} , of the orifice.

In these figures, it can be found in the good agreement between the estimations by the present theory and the experimental data of K. As for B, it is seen that the experimental data tend to deviate widely from the conventional theoretical estimations and that good agreement can be found between the estimations by the present theory and the experimental data.

From these results, it may be concluded that the present analysis yields the good predictions for the dynamic characteristics of bearings in a wide range of designing conditions.

6. Conclusions

The influence of the gas inertia forces generated within the stabilizing restrictor on the dynamic characteristics of externally pressurized circular thrust gas bearings with a stabilizer was examined theoretically and experimentally for the case when the flow of gas from the capillary restriction becomes turbulent. The stabilizer is inserted into the gas-supply line which consists of a fluid capacity and a capillary restriction. In consequence, the following conclusions have been obtained:

(1) The influence of the gas inertia forces is almost in agreement qualitatively with that in the first report. The influence can be determined by the inertia parameter, α , the compressibility parameter, β , and the Reynolds number, Re^*.

(2) The inertia effect is considerable

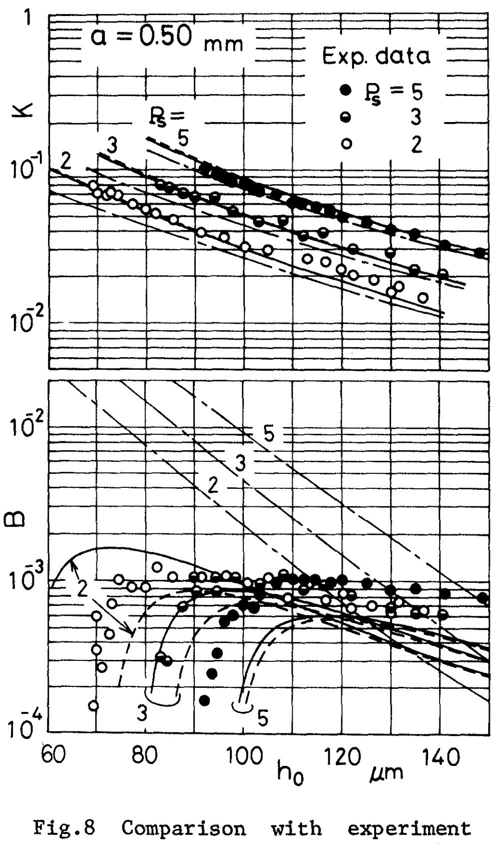

Fig.8 Comparison with experiment (Bearing 1)

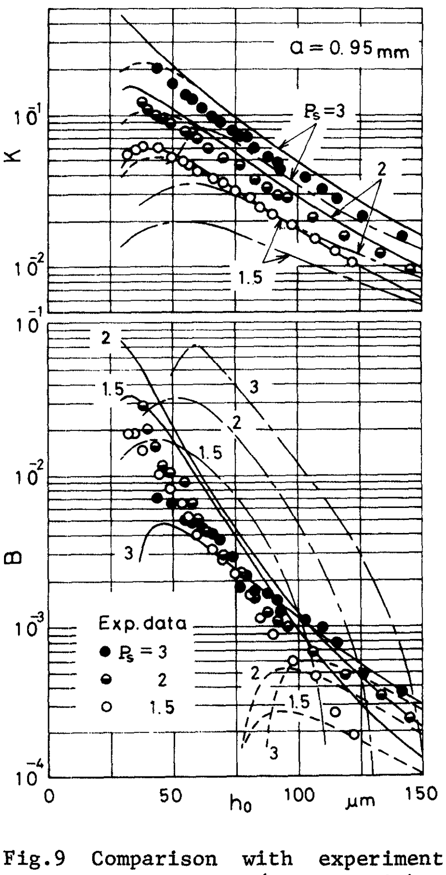

Fig.9 Comparison with experiment (Bearing 2)

when the feeding parameter, Γ, takes values for practical applications from 1 to 10. In general, the inertia effect on the damping coefficient is more remarkable than that on the stiffness.

(3) The inertia effect becomes remarkable as the Reynolds number, Re^*, decreases in value and as the inertia parameter, α, increases.

(4) The influence on the damping coefficient becomes significant as the supply pressure, P_s, increases in value. In general, however, the influence on the bearing stiffness hardly depends on P_s.

(5) The inertia effect becomes significant when the squeeze number, σ, decreases in value. In general, however, it is not so remarkable when σ is large.

References

(1) Haruyama, Y. and Mori, H., Bull. JSME , Vol.25, No.210 (1982-12)
(2) Haruyama, Y. and Mori, H., Proceedings of the Annual Meeting of JSME (in Japanese), No.804-6 (1980-3), p.29.
(3) Ohmi, M. and Usui, T., Bull. JSME, Vol.19, No.129 (1976-3), p.307.
(4) Perry, J. A., Trans. ASME, Vol.71 (1949), p.757.